Light scattering from vibrational modes in GaAs-$Ga_{1-x}Al_xAs$ superlattices and related alloys

J. Sapriel, J. C. Michel, and J. C. Tolédano
Centre National d'Etudes des Télécommunications, Laboratoire (No. 250) associé au Centre National de la Recherche Scientifique, 196 rue de Paris, F-92220 Bagneux, France

R. Vacher
Laboratoire de Spectrométrie Rayleigh-Brillouin, Equipe de recherche (No. 460) associée au Centre National de la Recherche Scientifique, Université des Sciences et Techniques du Languedoc, F-34060 Montpellier Cedex, France

J. Kervarec and A. Regreny
Centre National d'Etudes des Télécommunications, F-22301 Lannion, France
(Received 20 April 1983)

Raman and Brillouin scattering investigations are performed on GaAs-$Ga_{1-x}Al_xAs$ superlattices which have been fully characterized by means of x-ray diffraction. Six superlattice samples with periods ranging from 45 to 250 Å and with an aluminum concentration x around 0.3 have been investigated by means of conventional Raman scattering. A doublet of lines due to the superlattice effect appears on the spectra. These Raman lines of symmetry A_1 are located on either side of the theoretical value corresponding to the first folded mode at $k=0$ of the longitudinal-acoustic branch. The crystalline quality of the GaAs layers of the superlattices has also been studied through comparisons between disorder-activated transverse-acoustic modes and second-order Raman lines. Precise measurements on surface-acoustic-wave velocity have been performed by means of a high-contrast and high-sensitivity Brillouin experimental setup. Several $Ga_{1-x}Al_xAs$ epitaxial layers with $0<x<0.8$ have been studied and the velocity variations in the [100] and [110] directions have been determined. The elastic constants of $Ga_{1-x}Al_xAs$ undergo a small decrease with increasing values of x. Concerning the Brillouin measurements in GaAs-$Ga_{1-x}Al_xAs$ superlattices, the surface-wave velocities are slightly higher than in the corresponding mean homogeneous medium. Possible stresses in the alternating layers could be at the origin of this difference.

I. INTRODUCTION

Superlattice crystals are prepared by alternately depositing predetermined thicknesses d_1 and d_2 of two compounds. An artificial period $D=(d_1+d_2)$ is thus created in the direction perpendicular to the layers, which produces additional branches in the phonon dispersion curves and extra gaps in the folded Brillouin zone.[1-3] Until now, the vibrational studies have been performed mainly on GaAs-AlAs superlattices grown on the (001) face of a single-crystal GaAs substrate. In this paper we consider alternating GaAs-$Ga_{1-x}Al_xAs$ crystals with $0.25<x<0.40$. Obviously the perturbation of the phonon branches of the unlayered structure is smaller in this case, since only a fraction x of the Ga atoms are replaced by Al atoms. On the other hand, one can expect a better lattice matching between adjacent layers which could also lead to better crystalline properties. All the investigated superlattices had a relatively long period ($D>50$ Å) with respect to the interatomic distances. In order to clarify the properties of these superlattices it is of interest to examine the properties of related alloys.

In the case of $Ga_{1-x}Al_xAs$ alloys the long-wavelength optical phonons display a two-mode behavior.[4,5] Recently[6] their Raman spectra between 0 and 400 cm^{-1} have been carefully investigated throughout the whole composition range $0<x<1$.

To our knowledge, no experimental work has been published to date on the acoustical properties of III-V alloys and superlattices. Yet these properties are closely related to the optical phonons, especially the ones which result from the folding of the acoustic branches and which have appeared in all the investigated superlattices as shown in the Raman scattering part of the present study. Since these kinds of materials are obtainable only as thin samples, a few microns thick, they are not suitable for the study of bulk acoustic waves. By contrast the velocity of surface acoustic waves can be determined, because of the short penetration depth of these waves.

This paper is devoted to the experimental study of vibrations in GaAs-$Ga_{1-x}Al_xAs$ superlattices and in $Ga_{1-x}Al_xAs$ mixed crystals. Two techniques, the Raman and the Brillouin scattering have been used for this purpose.

In Sec. II an elastic model is applied to the above superlattices to determine the bulk phonon dispersion curves and the lowest frequency branches are approximated by an analytical formula. The x-ray characterization of the superlattices is then described. A Raman study between 0 and 400 cm^{-1} of these superlattices is reported which is mainly focused on the folding of the acoustic branches.

The elastic properties of $Ga_{1-x}Al_xAs$ mixed crystals and related superlattices are presented in Sec. III. They have been investigated through the surface-acoustic-wave

velocities whose values have been determined by means of Brillouin scattering.

Finally the set of results concerning the folding of the acoustic branches obtained by means of Raman scattering and the Brillouin scattering surface-acoustic-wave measurements in GaAs-$Ga_{1-x}Al_xAs$ superlattices and $Ga_{1-x}Al_xAs$ crystals, are discussed and a general conclusion is given (Sec. IV).

II. RAMAN SCATTERING INVESTIGATION IN GaAs-$Ga_{1-x}Al_xAs$ SUPERLATTICES AND THE FOLDING OF THE ACOUSTIC BRANCHES

A. Application of the elastic model to the determination of the phonon dispersion curves

Theoretical studies of bulk and surface vibrations in superlattices have been recently presented.[7,8] In Ref. 8 two methods of determination of the dispersion curves of bulk waves are compared, one based on the elasticity theory and the other derived from a linear-chain model of two alternating diatomic sublattices of GaAs and AlAs along [001]. It was established that for a number of monolayers of GaAs and AlAs larger than five per period, the two models give the same calculated values for the dispersion curves as long as the lowest energy branches are considered. As the present study is mainly focused on long period superlattices and on the first folded branches, we have chosen to use the elastic model which is easier to carry out. For alternating (001) layers, the symmetry of GaAs or $Ga_{1-x}Al_xAs$ ($\bar{4}3m$) is reduced to the point group $\bar{4}2m$. The translation symmetry is also lowered in the [001] direction, giving rise to the typical zone-folding effects represented in Fig. 1. Group theory shows that for an ideal crystal and in the case in which the wave vector is parallel to [001], there is a complete separation of transverse and longitudinal vibrations belonging to different irreducible representations (see Appendix I).

In a superlattice consisting of two alternating media of acoustic velocities v_1, v_2, and densities ρ_1 and ρ_2, the circular frequency ω and the wave vector k in the direction perpendicular to the layers, are related[9] by

$$\cos K=\cos\left[\frac{\Omega}{1+d_2/d_1}\right]\cos\left[\frac{\Omega}{1+d_1/d_2}\frac{v_1}{v_2}\right]-\frac{1+Z^2}{2Z}\sin\left[\frac{\Omega}{1+d_2/d_1}\right]\sin\left[\frac{\Omega}{1+d_1/d_2}\frac{v_1}{v_2}\right], \tag{1}$$

where we have introduced[8] the dimensionless variables $K=kD$, $\Omega=(\omega D)/v_1$, and $Z=(\rho_1 v_1)/(\rho_2 v_2)$. It is more convenient to represent K as a function of Ω, thus considering a standard folded Brillouin zone where the different phonon branches depend on the ratio d_1/d_2, v_1/v_2, ρ_1/ρ_2, but not on the period D of the superlattice. These branches are represented in Fig. 1, for a GaAs-AlAs superlattice with $d_1=d_2$, the first medium, taken as a reference, being GaAs. The acoustic properties of $Ga_{1-x}Al_xAs$ are unknown, but as the lattice parameters are very similar, one can take, to a good approximation, the same set of elastic constants for GaAs and $Ga_{1-x}Al_xAs$. The same dispersion curves K vs Ω are therefore valid for longitudinal modes (elastic constant C_{11}) as well as for transverse modes (C_{44}). The actual frequencies ω_L and ω_T of the longitudinal and transverse modes corresponding to a given point of the standard Brillouin zone (for example one of the zone-center M,N,P,Q points or one of the zone-edge S,T,U,V points) are clearly related by

$$(\omega_L/\omega_T)^2=C_{11}/C_{44}\ . \tag{2}$$

For GaAs, the value[10] of the ratio C_{11}/C_{44} is close to 2; Eq. (2) is valid for every GaAs-$Ga_{1-x}Al_xAs$ superlattice for $0<x<1$, irrespective of the layer thicknesses. One can easily notice that the frequencies ω_L,ω_T and the widths Δ of the different energy gaps are inversely proportional to the superlattice period D. For example, for $x=1$ and $d_1=d_2$, one finds at the M point: $\omega_L(\mathrm{cm}^{-1})D(\text{Å})=1700$; $\omega_T(\mathrm{cm}^{-1})D(\text{Å})=1200$, and for the first center-zone gap MN: $\Delta_L(\mathrm{cm}^{-1})D(\text{Å})=2.61$, $\Delta_T(\mathrm{cm}^{-1})D(\text{Å})=1.85$. For $x<0.4$ the gapwidths become so small that they can be neglected and one can obtain for the general form of the nth phonon branch the following equation:

$$\omega_n=V\left[(-1)^{n+1}k+\frac{2\pi}{D}E(n/2)\right], \tag{3}$$

where $E(n/2)$ is the integral part of $n/2$ and V is the bulk acoustical velocity in the direction perpendicular to the layers. For acoustic wavelength $\lambda\gg D$, one finds

$$\frac{1}{V}=\frac{1}{D}\left[\frac{d_1^2}{v_1^2}+\frac{d_2^2}{v_2^2}+\frac{d_1d_2}{v_1v_2}\left[Z+\frac{1}{Z}\right]\right]^{1/2}.$$

The first folded branch corresponds to $n=2$, the second folded branch to $n=3$, etc., in Eq. (3).

Symmetry considerations based on group theory show that the phonons at points M and N of Fig. 1 belong to the irreducible representations A_1 and $B_2(z)$ in the case of the longitudinal branch. Concerning the transverse-acoustic branch the phonons have the symmetries $E(y)$ and $E(x)$

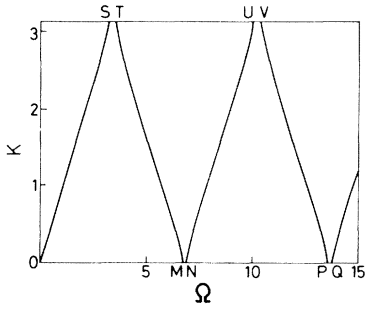

FIG. 1. Phonon dispersion branches for a propagation perpendicular to the layers (along z); $K=k_zD$ and $\Omega=(\omega D)/v_{GaAs}$. D is the GaAs-AlAs superlattice periodicity. M and N are the first GaAs folded acoustic modes; MN is the first gap at $k=0$. This representation is valid for longitudinal-acoustic vibrations [$v_{GaAs}=(C_{11}/\rho)^{1/2}$] and transverse-acoustic modes [$v_{GaAs}=(C_{44}/\rho)^{1/2}$]. The same thicknesses have been taken for GaAs and AlAs layers. The elastic constants and density of GaAs are taken from Ref. 10. The same elastic constants are taken for AlAs.

at points M and N. These results relative to the folded acoustic modes in the Brillouin-zone center, which were stated without proof in Refs. 1–3 are established in Appendix I of this paper, as well as the symmetry of the folded branches for $k_z \neq 0$.

B. Sample preparation and x-ray characterization of the superplattices

The GaAs-$Ga_{1-x}Al_xAs$ superlattices have been prepared on (001) oriented GaAs substrate by molecular-beam epitaxy and consist of alternating layers of GaAs and $Ga_{1-x}Al_xAs$ repeated a sufficient number of times to create crystals of micron dimensions. Let N_1 and N_2 be the number of monolayers of GaAs and $Ga_{1-x}Al_xAs$, respectively, in the superlattice period.

All superlattice samples investigated by means of Raman and Brillouin scattering were carefully characterized previously. X-ray diffraction in the vicinity of the (00l) Bragg reflection of the GaAs substrate allows the determination of the structural parameters d_1, d_2, and x. Diffraction angle measurements give the periodicity $D=(d_1+d_2)$ and the mean value $\bar{x}$ of the aluminum concentration in a superlattice unit cell,

$$\bar{x}=\frac{N_2 x}{N_1+N_2} .$$

From the knowledge of $\bar{x}$ and D, the structural parameters x, d_1, and d_2 are determined through an iterative method[12] where the theoretical and experimental structure factors are compared.

A typical x-ray diagram of a superlattice sample is give in Fig. 2(a). It was obtained with a powder goniometer fitted with a post sample quartz monochromator. The resolution of a double-crystal spectrometer allows the separation between the zero-order satellite of the superlattice and the substrate peak as shown in Fig. 2(b). One can also compare the linewidth of the Bragg reflection lines corresponding to the superlattice and the substrate. The narrowness of the superlattice peak is indeed clear evidence of the good crystalline quality. The x-ray diagrams of Figs. 2(a) and 2(b) have been obtained for a simple corresponding to $N_1=24$, $N_2=36$, and $x=0.38$. The homogeneity has been checked at different points of the sample. The variations of N_1 and N_2 are of the order of one monolayer (one monolayer corresponds to a thickness of $\simeq 2.83$ Å) across the sample.

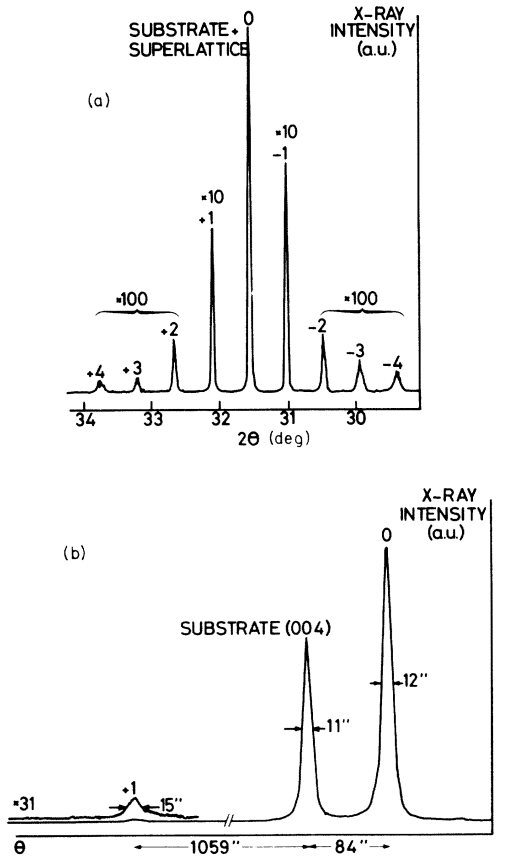

FIG. 2. X-ray diffraction diagrams in a GaAs-$Ga_{0.62}Al_{0.38}As$ superlattice with 24 monolayers of GaAs and 36 monolayers of GaAlAs in the period (sample V). θ is the diffraction angle. (a) Diagram in the vicinity of the (002) Bragg reflection of GaAs. The satellite 0 of the superlattice merges in the GaAs (002) peak. One can see the satellites $\pm 1, \pm 2, \pm 3, \pm 4$. The peak labeled 0 corresponds to the Bragg reflection (0,0,60). The intensities of peaks ± 1 have been reduced by 10 and that of peak 0 by 100. (b) High-resolution diagram in the vicinity of the (0,0,4) peak of GaAs. The zero-order peak which corresponds to the reflection (0,0,120) is well separated. The peak widths of the superlattice and the substrate are comparable.

C. Raman scattering results

The only experimental observation of the zone folding of acoustic branches has been reported by Colvard *et al.*[2,3] The first optical modes near $k=0$ of the folded Brillouin zone have been observed by means of resonant Raman scattering on GaAs-AlAs superlattices, each period being constituted of a few monolayers of GaAs and AlAs. The Raman resonance enhances appreciably the weak structures which otherwise could not be observed, but also modifies the Raman selection rules, bringing possible uncertainty in the interpretation of the spectral lines. Our measurements have been obtained far from resonance (which occurs for $\lambda > 7000$ Å in our samples), where the Raman selection rule is valid in crystals.[13] The experimental setup has been described before.[6] The samples were observed under vacuum in order to suppress spurious low-frequency Raman lines from atmospheric N_2 and O_2 rotational transitions. Three spectral ranges were of particular interest in our samples: below 40 cm^{-1} for the study of the folding of the acoustic branches, between 250 and 400 cm^{-1} for the investigation of the optical region, and between 50 and 240 cm^{-1} for the observation of broad structures due either to the second-order scattering or to disorder-activated modes.

Our Raman measurements have been performed in a backscattering arrangement along the $z=[001]$ direction and with the Ar^+-ion laser lines (4880 and 5145 Å). Several scattering geometries have been studied: (x,x), (x,y), $(x+y,x+y)$, and $(x+y,x-y)$. Here, (x,y) denotes incident light polarized along [100] and scattered along [010], and $(x+y,x-y)$ denotes incident light polarized along [110] and scattered along $[1\bar{1}0]$ in the point group

$\bar{4}2m$ of the superlattice. A_1 vibrations are expected to be seen in (x,x) and $(x+y,x+y)$ and are extinguished in (x,y) and $(x+y,x-y)$. The B_2 modes are expected to be observed in (x,y) and $(x+y,x+y)$ and should disappear in the (x,x) and $(x+y,x-y)$ configurations. Figure 3(a) shows a Raman spectrum of a superlattice sample ($d_1=d_2=54$ Å, $x=0.28$) at room temperature with the laser incident at the Brewster angle, giving an angle in the sample of $\sim 15°$ to the normal. The two lowest-frequency lines indicated by arrows are observed for the first time. They do not belong either to GaAs or to $Ga_{1-x}Al_xAs$ but are interpreted as being due to the superlattice. The symmetry of these lines is experimentally found to be A_1. The Stokes and anti-Stokes part of the low-frequency spectrum are reproduced on Fig. 3(b) and show that these lines correspond to inelastic scattering. The temperature behavior is that of first-order phonon scattering. The frequencies of these lines measured on six different samples (I–VI) with periods between 45 and 260 Å, are reported in Table I, column 6. This table also shows (column 5) the theoretical frequency of the first folded modes at $k=0$ corresponding to the longitudinal-acoustic branch calculated from Eq. (1). The approximate values of the transverse modes may be obtained by dividing by $\sqrt{2}$ according to Eq. (2). The values for the longitudinal-acoustic folded first modes, corresponding to Colvard's samples (A,B,C) are also given in Table I. The theoretical values are in this case calculated from Eq. (1), where we have taken the same value for the velocity of AlAs as in Ref. 2. It is worthwhile to note that column 5 contains two values associated to the points M and N for samples A,B,C even though there is only one value corresponding to samples I–VI for which the approximation given by Eq. (3) is valid because of the large value of the period D and the relative smallness of x which give negligible gapwidths.

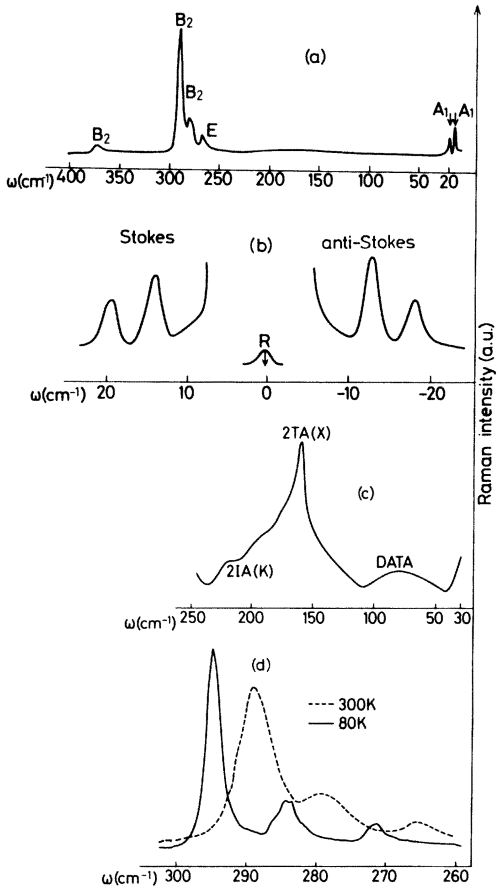

FIG. 3. Raman scattering in a GaAs-$Ga_{0.70}Al_{0.3}As$ superlattice with $d_1=d_2=54$ Å. (a) Typical Raman spectrum obtained at Brewster incidence. The incident light is polarized along [110] and the scattered one is collected for all polarizations. The symmetry of the vibrations are indicated. The new lines due to the superlattice are shown by arrows. (b) Stokes and anti-Stokes part of the low-frequency lines of the Raman spectra; R indicates the position of the Rayleigh line. (c) Second-order Raman 2TA and disorder-activated acoustic mode (DATA) which come from the unfolded Brillouin zone of GaAs. (d) GaAs and GaAs-like Raman lines at 300 and 80 K. In each spectrum the highest-frequency line is the LO and the lowest-energy one the TO of GaAs. The second line is the GaAs-like LO line in $Ga_{0.7}Al_{0.3}As$.

It is clear from Table I that the observed Raman lines are located on either side of the theoretical value of column 5 which corresponds to $k=0$. Let us consider now the phonon which is involved in the backscattering Raman process. Its wave vector $\vec{k}$ is equal to $4\pi n/\lambda$, λ being the laser wavelength and n the refractive index. The corresponding phonons in the first and second folded branches are separated by $\Delta\omega=2Vk$ according to Eq. (3). Expressed in cm^{-1}, $\Delta\omega$ is of the order[10] of 5 cm^{-1}, value which is approximately equal to the distance between the doublet lines reported in Table I, column 6. If the energy separation is well accounted for by the theory, there is a qualitative discrepancy concerning the symmetry of these lines which are both A_1 (instead of being A_1 and B_2 as dictated by group theory), if we consider that they arise at $k=0$. However, we can note that in the present case, we must consider the branches for $k_z\neq 0$. Actually the k vector of the phonon involved cannot be neglected with respect to the dimension π/D of the Brillouin zone even for Colvard's short-period superlattices. The role of the k-vector magnitude which is only implicit in the literature [see Fig. 2(b) of Ref. 2] has been pointed out by Jusserand *et al.*[14] who have experimentally determined several points of the dispersion curves of long-period superlattices by changing the laser wavelength. It is worthwhile pointing out that this doublet of A_1 lines is quite similar from one sample to another, the lower-frequency line being approximately 30% more intense. Both lines are very sharp. The observed half-widths at half maximum are less than 2 cm^{-1}.

As shown in the Appendix the A_1 and B_2 modes are related to two branches having the same symmetry for $k_z\neq 0$ and obeying the same selections rule which is identical to that of a $k=0$, A_1 mode, consistently with the experimental observation.

The folding of the transverse-acoustic branch gives no supplementary lines on the spectra since the folded modes are of a symmetry E forbidden in our experimental arrangement. It is also shown in the Appendix that this selection rule is preserved for $k_z\neq 0$ and prevents the observation of any transverse mode. These modes appeared at resonance[3] in Colvard's samples with frequencies ω_T checking Eq. (2) to a good approximation.

TABLE I. Experimental values of the Raman lines due to the first folding of the acoustical-longitudinal branch in the superlattices. *A,B,C* designate the samples investigated by Colvard *et al.* The two theoretical values correspond to the points *M* and *N* (see Fig. 1). In the case of our samples I–VI, the points *M* and *N* are too close to be distinguished within the experimental errors. The parameters d_1, d_2, and x of samples I–VI have been obtained by means of x-ray diffraction (Ref. 12). The lower-frequency line in case of sample VI is too close to the Rayleigh line and could not be observed. The theoretical values corresponding to samples I–VI are obtained from the values of elastic constants (Ref. 10) of GaAs. It is clear that the folding of the longitudinal-acoustic branch gives two Raman lines from both sides of the theoretical values. (Compare column 6 to 5.) The energy difference between the doublet lines is given by $2Vk$, V being the longitudinal-acoustic velocity in the superlattice and k the wave vector of the phonon involved in the light scattering process.

Sample	d_1 (Å)	d_2 (Å)	x	$\omega(cm^{-1})$ theor. zone-center first folded modes	$\omega(cm^{-1})$ expt. Raman lines	Reference
A	13.6	11.6	1	63.8–65.9	63.1–66.9	Colvard
B	20.7	12.4	1	47.4–50.8	52–57	*et al.*
C	26.6	10.9	1	41.2–44.8	39–45	
I	24±3	24 ±3	0.3 ±0.02	33.5	32–37	
II	48±3	28.3±2	0.28±0.02	21.0	18.2–22.3	This
III	54±3	54±3	0.28±0.02	15.0	13.4–19.2	work
IV	54±3	79±3	0.36±0.02	12.5	10.5–15.4	for
V	68±1.5	102±1.5	0.38±0.005	9.5	8–13	$\lambda=5145$ Å
VI	150±3	107±3	0.36±0.01	6.25	?–10	

In our superlattices where the thickness of the layers is large with respect to the interatomic distances, the frequency of the optical phonons in GaAs and $Ga_{1-x}Al_xAs$ is scarcely modified. The peaks at 291 and 267.5 cm^{-1} [see Fig. 3(a)] are, respectively, the LO and TO of GaAs. The TO of *E* symmetry results from a "leakage" due to the departure of strict 180° backscattering and is observable in (x,x) and (x,y). The peaks at 280 and 376 cm^{-1} are attributed to the GaAs-like and AlAs-like LO modes in $Ga_{1-x}Al_xAs$. Their frequency is related[6] to the Al concentration x. We have not observed any folded mode in the optical region. Probably due to the lack of dispersion of the optical branches and the long-period D along z, these weak modes are too close to the unfolded modes to be distinguished, even at low temperatures when the Raman lines become narrow, thus reducing the possibility of overlapping. All LO peaks in the superlattice appear only in (x,y) and $(x+y,x+y)$ the symmetry assignment being $B_2(z)$. These modes in bulk GaAs and AlAs appear in the same scattering arrangement, but in $F_2(z)$ symmetry of $\bar{4}3m$.

When the slit apertures of the monochromator are large enough ($\simeq$500 μm), one can observe weak and broad Raman structures between 30 and 250 cm^{-1} which can be attributed to the disorder-activated transverse-acoustic mode[6] (DATA) around 80 cm^{-1} and to the second-order 2TA in GaAs [Fig. 3(c)] at the zone edge of the unfolded Brillouin zone. The intensity of the DATA being clearly less than the intensity of the second-order 2TA, one can conclude that the disorder in the GaAs layers is quite small (actually the spectra are very similar to chemically etched GaAs substrates). The good crystalline quality of the superlattice has been also controlled by the high degree of polarization of the Raman lines, by the observation of a quite low scattered background, and the strong narrowing of the Raman lines when the temperature is lowered from room temperature toward 80 K (Fig. 3(d)].

III. STUDY OF THE LONG-WAVELENGTH ACOUSTIC MODES

A. Analysis of the existing experimental methods

Raman scattering allows the observation of only short-wavelength acoustic modes[13] through the double-phonon interaction process. Acoustic modes can be studied with a poor precision along the whole Brillouin zone by means of neutron scattering. This technique fails in the case of thin epitaxial layers because the interaction volume is too small. Ultrasonic techniques and Brillouin scattering are accurate techniques to determine the zone-center acoustic-mode properties which are fully characterized by the determination of the set of elastic constants c_{ij} and the acoustic attenuation.

Ultrasound are produced up to 1 GHz by piezoelectric transducers[15] and for the determination of bulk acoustic properties crystal volumes of a few mm^3 are needed. In the case of thin layers, ultrasonic techniques with suitable wedge or interdigital transducers can be used to study surface waves provided that the film thickness is larger than the acoustic penetration depth to avoid interference with the substrate. For samples of around 1 μm thickness which are available in the laboratory, Brillouin scattering by surface thermal phonons is the only accurate method.[16] It is also a versatile and nondestructive tool which can be used successfully for absorbing crystals such as semiconductors GaAs and Si as well as for totally opaque metals. Concerning the bulk acoustic waves, Brillouin scattering gives rise to broad lines[17] which originate from the contribution of phonons within the wave-vector range $\Delta k \simeq \alpha$, α being the absorption coefficient of the exciting laser beam. These lines allow less precise velocity measurements than the very sharp Brillouin lines associated to the surface acoustic waves.

TABLE II. Calculated velocities of the Rayleigh waves and the pseudo-surface-waves in GaAs. The elastic constants have been taken from Ref. 10. θ is the angle between the wave-propagation vector and the [100] direction in the (001) plane.

θ (degrees)	0	5	10	15	20	25
Rayleigh wave velocities (m/s)	2711	2717	2725	2732	2747	2747

θ (degrees)	30	35	40	45
Pseudo-surface-wave velocities (m/s)	2830	2837.5	2845	2856

B. Surface waves in cubic crystals and superlattices

Rayleigh surface waves (RSW) are modes of propagation of elastic energy along the free boundary of an infinite half-space. The amplitude of their displacement undergoes an exponential decay with depth below the free surface and vanishes within a distance of the order of two wavelengths. The reader is referred to Farnell for a review of the properties of Rayleigh surface waves.[18]

Let us consider the RSW propagation in the (001) plane of a cubic crystal such as GaAs in a direction making an angle θ with [100]. For $\theta=0$ the vibration is polarized in the sagittal plane (which contains the k vector and the normal to the surface). When θ increases this polarization becomes gradually transverse. In the case of GaAs and for a value $\theta\simeq 27°$ the RSW merges in the bulk transverse wave BT_1 polarized in the (001) plane. For $\theta\simeq 25°$, a new kind of vibration appears associated to a pseudo-surface-wave (PSW) whose displacement amplitude undergoes a decay also in the propagation direction due to the scattering by BT_1 modes. For increasing values of θ, the coupling strength between PSW and BT_1 becomes weaker and completely vanishes for $\theta=45°$, for which the PSW actually becomes a real surface wave. For GaAs the calculations[19] give for the velocity of the RSW and the PSW the values indicated in Table II. These velocities are clearly slowly varying functions of the angle θ.

The velocities v_s of the surface waves in a cubic crystal are given by[20]

$$C_{11}\left[v_s^2-\frac{C_{44}}{\rho}\right]\left[v_s^2-\frac{C_{11}}{\rho}+\frac{C_{12}^2}{C_{11}\rho}\right]^2=C_{44}v_s^4\left[v_s^2-\frac{C_{11}}{\rho}\right], \tag{4}$$

$$C_{11}\left[v_s^2-\frac{C_{44}}{\rho}\right]\left[v_s^2-\frac{2C_{44}+C_{12}+C_{11}}{\rho}+\frac{C_{12}^2}{C_{11}\rho}\right]^2=C_{44}v_s^4\left[v_s^2-\frac{2C_{44}+C_{12}+C_{11}}{\rho}\right]. \tag{5}$$

Equations (4) and (5) which are of third degree in v_s^2 refer to the [100] and [110] propagation directions, respectively. They contain the three independent elastic constants of the crystal.

Bulk sound propagation has been theoretically studied in superlattices made of two alternating isotropic media. For long wavelengths ($\lambda\gg D$) the system behaves as an hexagonal homogeneous crystal and explicit expressions for the complete set of five independent elastic constants have been found in terms of the thickness, the density, and the elastic constants of the two constituents.[21] In the case in which the media are cubic, the superlattice is equivalent to a tetragonal crystal whose effective-elastic-constant expressions have not been determined yet. Only the two constants C_{11}^{eff} and C_{44}^{eff} relative to the propagation along the [001] axis can be obtained easily since their expressions do not differ from the case of superlattices composed of isotropic layers.

C. Brillouin scattering measurements of surface wave velocity

A Brillouin spectrometer using a triple-pass plane and confocal Fabry-Perot interferometers in tandem has been constructed in our laboratory. The frequency resolution is 10^8 and the contrast is of the order of 10.[10] This spectrometer is suitable for the study of light scattering from surface acoustic waves. The whole system is controlled and stabilized by a HP 9825 calculator. The principle of operation and the optical arrangement are very similar to those described in Ref. 22.

The triple-pass plane Fabry-Perot is used like a filter whose maximum transmission is adjusted and maintained on the frequency of the Brillouin line under investigation owing to an additional reference line which is transmitted at the same position as the Brillouin line but is intense enough to allow automatic adjustment of the maximum

transmission of the plane Fabry-Perot interferometer. This reference line is generated with the help of an electro-optic modulator at the frequency of the Brillouin line.[23]

Fast repetitive scanning of the confocal Fabry-Perot interferometer is performed to eliminate the broadening of the Brillouin lines due to slow frequency drifts originating from thermal fluctuations. The luminosity and sensitivity of the whole system are high enough for the recording of Brillouin lines whose intensity is of the order of a few counts per second on the photomultiplier. The free spectral range was 25 and 1.48 GHz for the plane and confocal Fabry-Perot interferometers, respectively. The 4880-Å single-mode argon-ion laser radiation was polarized in the plane of incidence and focused with a 15-cm focal length lens upon the sample. Powers lower than 400 mW were used to prevent local heating. The scattering geometry is given in Fig. 1 of Ref. 16. We kept $\theta_s-\theta_i$ fixed at 22° (θ_s and θ_i are scattering and incident angles, respectively) and varied θ_s between 45° and 55°. No analyzer was used in the scattered beam.

We have measured the velocity of the surface acoustic waves in the two directions $\theta=0°$ and 45° in $Ga_{1-x}Al_xAs$ alloys for $0<x\ll 0.8$ and in three of the superlattices of Table I. Only samples of excellent surface quality were investigated, since the others gave Brillouin spectra with a signal-to-noise ratio too weak to allow precise measurements.

The wave-vector conservation requirement[16] gives for the wave number $K=\omega/v_s$ of the surface wave,

$$K=k_i\sin\theta_i+k_s\sin\theta_s\ , \tag{6}$$

k_i and k_s being the wave numbers of incident and scattered light, respectively. In our experimental conditions the wavelengths of the acoustic waves under investigation ranged from 2700 to 3000 Å according to θ_i values.

The velocity v_s of the surface waves along the [100] and [110] directions of the (001) free surface have been measured with our experimental setup in $Ga_{1-x}Al_xAs$ epitaxial layers of several micrometers thickness which had been grown by liquid-phase epitaxy on a (001) substrate. The $Ga_{1-x}Al_xAs$ crystals were of the n or p type, the carrier concentration being less than 5×10^{17} cm^{-3}. The values of x were determined by electron microprobe analysis with an uncertainty Δx of the order of 0.02. The experimental results are plotted (Fig. 4) in full lines. The uncertainty on the surface-wave-velocity measurements is about ±0.5%. One can notice that the experimental v_s values in GaAs (2690 and 2817 m/s in [100] and [110], respectively) are in good agreement with the calculated values from elastic

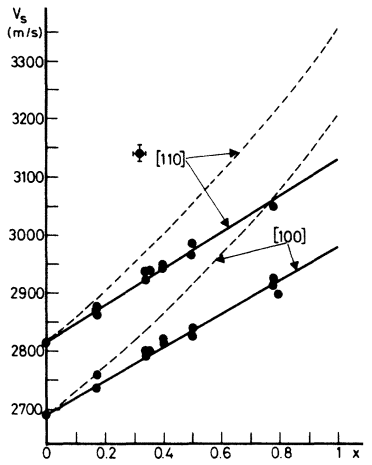

FIG. 4. Surface-acoustic-wave velocities vs the concentration x in $Ga_{1-x}Al_xAs$ epitaxial layers. The full lines join the experimental points; the broken lines are calculated curves obtained by keeping the same set of elastic constants (Ref. 10) for all x values.

constants[10] reported in Table II. The velocity variations versus x plotted in Fig. 4 can be approximated by the following linear laws:

$$v_s=2690+290x$$

along [100] and

$$v_s=2817+315x$$

along [110].

In Fig. 4 one can find also the theoretical velocity variations (dashed lines) in the case where the elastic constants are kept constant versus x and where only the density variations are taken into account. One easily finds for both [100] and [110] directions,

$$v_s(x)=v_s(0)[144.64/(144.64-42.72x)]^{1/2}\ .$$

Here $v_s(0)$ are the corresponding measured values in GaAs. From comparison between full and dashed lines, one can notice the tendency of the elastic constants to softening, which results from substitution of Ga by Al in the gallium atomic sublattice. However, for the gallium-rich samples ($x<0.40$), taking the same constants set for the c_{ij} in $Ga_{1-x}Al_xAs$ as in GaAs is a rather good approximation, according to our Brillouin experimental results. The surface velocity curves plotted in Fig. 4 can be used to determine the x value of unknown samples with an uncertainty $\Delta x=0.05$.

TABLE III. Acoustic properties of GaAs-$Ga_{1-x}Al_xAs$ superlattices. The samples are labeled in the same way as in Table I. $\bar{x}=(xd_2)/(d_1+d_2)$ is the mean aluminum concentration. $\bar{v}_s$ are the surface velocities corresponding to $\bar{x}$ expressed in m/s in the [100] and [110] directions, which are taken from Fig. 4. v_s are the surface acoustic velocities which result from our Brillouin scattering measurements.

Superlattice	$\bar{x}$	$\bar{v}_s$[100]	$\bar{v}_s$[110]	v_s[100]	v_s[110]
III	0.14	2730	2860	2747.0	2900
IV	0.215	2750	2880	2777.5	2927
V	0.225	2755	2885	2760.0	2907

The sample spectrometer with identical experimental conditions was used to investigate the acoustic properties of superlattices. Three samples out of six have been selected for their good surface quality. The results are reported in Table III. The characteristics of superlattices labeled II, IV, and V are indicated in Table I. In column 2 of Table III we report the mean aluminum concentration $\bar{x}=d_2x/(d_1+d_2)$, i.e., the aluminum concentration in an homogeneous material with the same thickness as the superlattice and containing the same number of Al, Ga, and As atoms. The surface velocities corresponding to $\bar{x}$ in both [100] and [110] directions are determined from the experimental curves of Fig. 4 and reported in Table III, columns 3 and 4. The corresponding measured values in the superlattices are given in columns 5 and 6. The measurements have been repeated several times to obtain a good accuracy. From Table III one can notice that the velocities are slightly higher in the superlattices than in the corresponding $Ga_{1-x}Al_xAs$ alloys. This difference seems to be larger than the experimental uncertainty and is probably due to a slight change in the elastic behavior between layers of several micrometers thickness (as in the epitaxial $Ga_{1-x}Al_xAs$ layers) and layers of several tenths of angstroms. This is supported also by the fact that for sample IV ($d_1=54$ Å, $d_2=79$ Å) the deviation is larger than for sample V ($d_1=68$ Å, $d_2=102$ Å) although the two samples have very close $\bar{x}$ values. One possible cause of the small enhancement of the elastic constants in superlattices is the presence of stresses due to the small difference between lattice parameters in GaAs and $Ga_{1-x}Al_xAs$ crystals. In $Ga_{1-x}Al_xAs$ epitaxial layers of several micrometers thickness, the stresses which are localized specially in the interface, can relax at the free boundary of the $Ga_{1-x}Al_xAs$ layers.

IV. DISCUSSION AND CONCLUSION

This paper, which deals with light scattering from bulk and surface vibrations in $Ga_{1-x}Al_xAs$ superlattices, is mainly focused on the properties of the acoustic modes: long-wavelength surface acoustic waves of the Rayleigh type and additional optical modes in the Brillouin zone due to the folding of the acoustic branches. The surface acoustic waves are studied by means of a high-contrast, high-resolution, and high-sensitivity Brillouin experimental setup while the additional modes due to the zone folding are investigated by means of a triple Raman monochromator allowing the observation of weak lines at energies as low as 5 cm^{-1}. These light scattering studies have been performed away from resonance. In the case of Raman scattering this leads to unambiguous assignments for the symmetry of the observed modes. A doublet appears in the Raman spectra of GaAs-$Ga_{1-x}Al_xAs$ superlattices which clearly corresponds to the folding of the longitudinal-acoustic branches, since the two components of the doublet are situated at a distance of a few cm^{-1} on either side of the expected frequency at $k=0$ of the first folding of these branches. The identical symmetry A_1 of the two lines has been shown to be due to the probing of the branches at $k_z\neq 0$.

Brillouin scattering measurements on $Ga_{1-x}Al_xAs$ epitaxial layers have been performed in two high-symmetry directions. The surface-wave acoustic-velocity variations show a slight softening of the set of elastic constants with increasing x values. Yet the behavior of each elastic constant has not been determined independently of the others, a supplementary relation between the three elastic constants being needed. A slight enhancement of the surface velocities in the superlattices with respect to the predicted ones, can be explained by the assumption that the elastic properties of thin layers (~ 50 Å) are different from the bulk. This hypothesis should be checked with short period superlattices before trying to give physical interpretation of the phenomenon. The presence of stresses in the superlattice layers is a possible explanation.

Let us conclude by a general remark. The problem of the large number of interfaces encountered by the propagating vibrations in the superlattices has not been touched upon in this paper. Actually they can play a significant role by breaking the periodicity and modifying the elastic properties of the media at their vicinity. The equations and models used are simplifications as they treat perfect homogeneous layers with perfect interfaces. They are nevertheless a first approximation adapted to this experimental work which presents the first systematic light scattering measurements from phonons in GaAs-$Ga_{1-x}Al_xAs$ superlattices and related compounds.

ACKNOWLEDGMENTS

The authors are indebted to B. Djafari-Rouhani and O. Hardouin du Parc for fruitful discussions on surface acoustic waves and to I. Abram and Y. Ballini for a careful reading of the manuscript and comments. They also wish to thank F. Bonnouvrier for numerical computations.

APPENDIX: SYMMETRY OF THE "FOLDED" ACOUSTIC BRANCHES

1. Symmetry of the folded modes at $k=0$

The taking into account of a Brillouin-zone folding when relating the properties of superlattice layers to those of the homogeneous bulk compound relies on the implicit assumption that the two structures are related by symmetry. Actually the symmetry group of the $Ga_{1-x}Al_xAs$-GaAs superlattice is a subgroup of $F\bar{4}3m$, involving a lowering of both the point symmetry (tetragonal) and the translational one (change of the lattice periodicity). On a macroscopic scale the structural change can be considered as a small effect as shown by the weakness of the additional Raman lines, and also by the weakness of the Bragg satellites in the x-ray spectrum, as compared the zeroth-order line (Fig. 2).

This suggests the possible use for working out the Raman activation of the acoustic branches of group-theoretical methods well established in the field of structural-phase transitions.[24] Here the continuously vanishing order parameter should be related to the vanishing of x in the alloy formula. We therefore adopt this assumption and consider the symmetry of the superlattice structure as the result of a "symmetry breaking" from the $F\bar{4}3m$ space group induced[25] by an irreducible representation Γ_n (k_z^*) (Ref. 26) of the former space group. The $\vec{k}_z$ vector representative of the star k^* of the representation is associated with the superlattice periodicity by

$\vec{k}_z \cdot \vec{D} = 2\pi$,

D being the superlattice period along [001]. For $D=(m+n)a/2$ (a being the lattice constant of the GaAs cubic lattice) we have $k_z=(4\pi)/[(m+n)a]$.

Standard group-theoretical methods[24] provide us straightforwardly with the matrices of the irreducible representations corresponding to $\vec{k}_z$. Four representations exist associated with the four distinct representations of the point group $mm2$, which is the invariance group of $\vec{k}_z$. However, the ambiguity on the one to use is entirely lifted if we assume the aluminum atoms to be uniformly distributed in the $Ga_{1-x}Al_xAs$ layers. Restricted to the elements of the $\bar{4}2m$ group, and to the $(\pm\vec{k}_z)$ arms of the star of $\vec{k}_z$, these matrices are

$$\begin{bmatrix} 1 & 0 \\ 0 & 1 \end{bmatrix}$$

for the elements $(E \mid 0)$, $(U_z \mid 0)$, $(\sigma_{xy} \mid 0)$, $(\sigma\bar{x}y \mid 0)$, and $(\vec{a}_1+\vec{a}_2)/2$,

$$\begin{bmatrix} 1 & 0 \\ 0 & -1 \end{bmatrix}$$

for the elements $(U_x \mid 0)$, $(U_y \mid 0)$, $(S_4 \mid 0)$, $(S_4^3 \mid 0)$, and

$$\begin{bmatrix} \cos\frac{2\pi}{m+n} & \sin\frac{2\pi}{m+n} \\ -\sin\frac{2\pi}{m+n} & \cos\frac{2\pi}{m+n} \end{bmatrix}$$

for the translations $(\vec{a}_2+\vec{a}_3)/2$ and $(\vec{a}_1+\vec{a}_3)/2$.

The possible symmetries of the superlattice structure corresponds to the invariance group of directions in the space spanning the representation. If we only focus on tetragonal space groups this procedure provides us with the desired space group of the superlattice structure.

For $(m+n)$ even we find $P\bar{4}m2$ (D_{2d}^5), the primitive translations being $(\vec{a}_1+\vec{a}_2)/2$, $(\vec{a}_2-\vec{a}_1)/2$, and $(m+n)\vec{a}_3/2$. For $(m+n)$ odd we obtain $I\bar{4}m2$ (D_{2d}^9), the primitive translations being $\vec{a}_2/2+(m+n)\vec{a}_3/2$, $(\vec{a}_2/2-(m+n)\vec{a}_3/2$, and $\vec{a}_1/2-(m+n)\vec{a}_3/2$.

These assignments differ from those of Ref. 27 where the groups $P\bar{4}2m$ (D_{2d}^1) and $I\bar{4}2m$ (D_{2d}^{11}) were found on the basis of structural considerations. The former authors obviously overlooked the fact that the mirrors of the superlattice structure are parallel to the vectors of the tetragonal unit cell.

Let us now consider the symmetry of the acoustic branches. In the GaAs structure, and for the $\vec{k}_z$ direction considered, these branches have symmetry properties which can also be described by irreducible representations of $F\bar{4}3m$. Under the operations of the $mm2$ invariance group of $\vec{k}_z$ the longitudinal displacement is totally symmetric, while the pair of transverse branches decomposed into nonsymmetric representations which are complex conjugated to each other. It is important to note that both the modes at $(+\vec{k}_z)$ and at $(-\vec{k}_z)$ are brought back to $\vec{k}=0$, in the superlattice, by the Brillouin-zone folding. The nondegenerate longitudinal branch therefore gives rise to two optic modes of the superlattice structure, and the degenerate transverse branch to four optic modes. The symmetry of these modes can be worked out by using a standard procedure[24,28] which consists of decomposing the irreducible representations of $F\bar{4}3m$ corresponding to the acoustic branches at $\vec{k}_z$ into the irreducible representations of $P\bar{4}m2$ or $I\bar{4}m2$ at $\vec{k}=0$.[29] One then finds the following relabeling of modes, which holds for both $(n+m)$ even or odd:

longitudinal modes:

$$(+\vec{k}_z, -\vec{k}_z) \rightarrow (A_1+B_2) \quad (\vec{k}=0,\ \bar{4}m2) ,$$

transverse modes:

$$(+\vec{k}_z, -\vec{k}_z) \rightarrow (E+E) \quad (\vec{k}=0,\ \bar{4}m2) .$$

2. Symmetry of the folded acoustic branches for $k_z \neq 0$

We are now able to deduce the symmetry of the folded acoustic branches for $k_z \neq 0$. These symmetries are labeled by irreducible representations of the space groups $P\bar{4}m2$ or $I\bar{4}m2$ corresponding to a wave vector $k_z \neq 0$. As these two groups are symmorphic these representations can be associated to the invariance point group of $\vec{k}_z$ which is $mm2$. We label the four types of representations $\Gamma_{k_z}(\tau_i)$, where τ_i is one of the four representations of $mm2$.

The symmetries of the folded acoustic branches can then be identified by having $k_z \rightarrow 0$. For the two longitudinal modes $\Gamma_{k_z}(\tau_i)$ must tend towards A_1 and B_2 while for the transverse ones it must tend towards E. In this identification it is only necessary to consider the characters of the representations with respect to the elements of the point group $mm2$. It is then easily found that A_1 and B_2 are associated with the same representation $\Gamma_{k_z}(\tau_1)$ where τ_1 is the totally symmetric representation of $mm2$. On the other hand, E is associated with $\Gamma_{k_z}(\tau_3)+\Gamma_{k_z}(\tau_4)$ where τ_3 and τ_4 are the two nonsymmetric representations of $mm2$ with character (-1) for U_z.

Owing to *their totally symmetric character* for $k_z \neq 0$ the A_1 and B_2 modes will behave like a Brillouin-zone-center A_1 mode and *have the same selection rules.* However, their intensities must have a different k dependence in the (x,x) Raman configuration since the mode tending towards B_2 is expected to have a vanishing intensity for $k_z \rightarrow 0$. As for the $\Gamma_{k_z}(\tau_3)$ and $\Gamma_{k_z}(\tau_4)$ modes they are expected to be allowed, respectively, in the (x,z) and (y,z) Raman configurations and remain therefore forbidden in the adopted backscattering arrangement.

[1] A. S. Barker, Jr., J. L. Merz, and A. G. Gossard, Phys. Rev. B 17, 3181 (1978).

[2] C. Colvard, R. Merlin, and M. V. Klein, Phys. Rev. Lett. 45, 298 (1980).

[3] C. Colvard, R. Merlin, and M. V. Klein, J. Phys. (Paris) Colloq. 42, C6-631 (1981).

[4] A. S. Barker and A. J. Sievers, Rev. Mod. Phys. 47, S2 (1975), and references therein.

[5]R. Tsu, H. Kawamura, and L. Esaki, in *Proceedings of the Eleventh International Conference on the Physics of Semiconductors, Warsaw, 1972,* edited by M. Miasek (P.W.N.-Polish Scientific, Warsaw, 1972), p. 1135.

[6]B. Jusserand and J. Sapriel, Phys. Rev. B 24, 7194 (1981).

[7]B. Djafari-Rouhani, L. Dobrzynski, and O. Hardouin du Parc, in The Third International Conference on Vibrations at the Surface, Asilomar, 1982 [J. Electron. Spectrosc. Relat. Phenom. 30, 119 (1983)].

[8]J. Sapriel, B. Djafari-Rouhani, and L. Dobrzynski, in The Fifth European Conference on Surface Science, Ghent, 1982 [Surf. Sci. 126, 197 (1983)].

[9]S. M. Rytov, Akust. Zh. 2, 71 (1956) [Sov. Phys.—Acoust. 2, 68 (1956)].

[10]Landolt-Bornstein, *Elastic, Piezoelectric and Related Constants of Crystals* (Springer, Berlin, 1979).

[11]M. Baudet, O. Regreny, G. Dupas, P. Auvray, M. Gauneau, A. Regreny, and G. Talalaeff. Mat. Res. Bull. 18, 123 (1983).

[12]J. Kervarec *et al.* (unpublished).

[13]R. Loudon, Adv. Phys. 13, 423 (1964). See also W. Hayes and R. Loudon, *Scattering of Light by Crystals* (Wiley, New York, 1978).

[14]B. Jusserand, D. Paquet, J. Kervarec, and A. Regreny (unpublished).

[15]J. Sapriel, *Acousto-optics* (Wiley, New York, 1979).

[16]J. R. Sandercock, Solid State Commun. 26, 547 (1978).

[17]J. R. Sandercock, Phys. Rev. Lett. 28, 237 (1972).

[18]G. W. Farnell, *Physical Acoustics* (Academic, New York, 1973), Vol. 6, p. 109.

[19]O. Hardouin du Parc (private communication).

[20]E. Sanz-Velasco, O. Hardouin Duparc, and V. R. Velasco, Surf. Sci. 126, 202 (1983).

[21]E. Behrens, J. Acoust. Soc. Am. 42, 378 (1967).

[22]R. Vacher, H. Sussner, and M. V. Schikfus, Rev. Sci. Instrum. 51, 288 (1980).

[23]H. Sussner and R. Vacher, Appl. Opt. 18, 3815 (1979).

[24]J. Petzelt and V. Dvorak, J. Phys. C 9, 1571 (1976).

[25]J. C. Tolédano and P. Tolédano, Phys. Rev. B 21, 1139 (1980).

[26]G. Y. Lyubarskii, *The Application of Group Theory in Physics* (Pergamon, New York, 1960).

[27]W. Andreoni and R. Car, Phys. Rev. B 21, 3334 (1980).

[28]J. C. Tolédano, Phys. Rev. B 19, 1147 (1979).

[29]D. R. Moore, V. J. Tekippe, A. K. Ramdas, and J. C. Tolédano, Phys. Rev. B 27, 7676 (1983).